Hindawi
Journal of Chemistry
Volume 2017, Article ID 2069519, 10 pages
https://doi.org/10.1155/2017/2069519

Research Article

Adsorptive Removal of Benzene and Toluene from Aqueous Environments by Cupric Oxide Nanoparticles: Kinetics and Isotherm Studies

Leili Mohammadi,[1] Edris Bazrafshan,[1] Meissam Noroozifar,[2] Alireza Ansari-Moghaddam,[1] Farahnaz Barahuie,[3] and Davoud Balarak[1]

[1]*Health Promotion Research Center, Zahedan University of Medical Sciences, Zahedan, Iran*
[2]*Analytical Research Laboratory, Department of Chemistry, University of Sistan and Baluchestan, Zahedan, Iran*
[3]*Engineering Faculty, Sistan and Baluchestan University, Zahedan, Iran*

Correspondence should be addressed to Edris Bazrafshan; ed_bazrafshan@yahoo.com

Received 11 May 2017; Revised 12 June 2017; Accepted 15 June 2017; Published 18 July 2017

Academic Editor: Nicolas Roche

Removal of benzene and toluene, as the major pollutants of water resources, has attracted researchers' attention, given the risk they pose to human health. In the present study, the potential of copper oxide nanoparticles (CuO-NPs) in eliminating benzene and toluene from a mixed aqueous solution was evaluated. For this, we performed batch experiments to investigate the effect of solution pH (3–13), dose of CuO-NPs (0.1–0.8 g), contact time (5–120 min), and concentration of benzene and toluene (10–200 mg/l) on sorption efficiency. The maximum removal was observed at neutral pH. By using the Langmuir model, we measured the highest adsorption capacity to be 100.24 mg/g for benzene and 111.31 mg/g for toluene. Under optimal conditions, adsorption efficiency was 98.7% and 92.5% for benzene and toluene, respectively. The sorption data by CuO-NPs well fitted into the following models: Langmuir, Freundlich, Temkin, and Dubinin-Radushkevich model. The experimental information well fitted in the Freundlich for benzene and Langmuir for toluene. Based on the results, adsorption followed pseudo-second-order kinetics with acceptable coefficients. The findings introduced CuO-NPs as efficient compounds in pollutantsadsorption. In fact, they could be used to develop a simple and efficient pollutant removal method from aqueous solutions.

1. Introduction

Benzene and toluene are widely used as solvents for organic compounds, cleaning equipment, and other downstream processes in the industry. They can enter the groundwater due to leakage from storage tanks, pipes, and improper burial sites [1, 2]. US Environmental Protection Agency (EPA) has introduced these compounds as primary pollutants with adverse effects on human health. They are also classified as carcinogen with definite carcinogenic properties [3, 4].

Toluene is suspected to disrupt the central nervous system and is classified as a Group E carcinogen. Given these health effects, EPA has announced the maximum pollution level of benzene and toluene in drinking water as 5 μg/L and 2 μg/L, respectively. Also according to US Public Health Service announcement in 1989, the amount of toluene in drinking water should not exceed 2 μg/L [5, 6]. Benzene and toluene are mostly found in effluents of chemical industries and refineries and have a high potential for pollution of surface water and groundwater. In addition, due to health effects, they are considered high-risk compounds for the environment [7]. Therefore, it is necessary to remove these compounds from water resources, particularly from surface water and groundwater.

Recently, nanoparticles (NPs) have been highly regarded by researchers for removal of pollutants. The unique properties of NPs and their high efficiency in removal of metals have made many researchers synthesize and use these substances for removal of environmental pollutants [8–10]. NPs have very good efficiency in the adsorption processes, especially

adsorption of metal pollutants, due to their large effective surface and many active sites. In addition, these adsorbents have been used on a large scale to improve the capacity of adsorption of compounds with specific functional groups [11]. Nanoscale metal oxides have the potential to save water treatment costs and given their size and high absorption efficiency, they can improve the efficiency of technologies [12, 13].

Copper oxide NPs (CuO-NPs) have been used as effective adsorbents of metals including arsenic, because there is no need to correct pH or oxidize arsenic 3 to arsenic 5, and they act very well in comparison with other NPs containing anionic compounds. According to studies of Martinson and Reddy [14], CuO-NPs are known to be effective in the removal of a large number of compounds.

Benzene and toluene elimination from groundwater resources has been widely studied using various processes, mainly in biological recovery, evaporation, oxidation, and adsorption processes. In previous studies, benzene and toluene adsorption by resin, crude and refined diatomaceous earth, and organoclay have been evaluated [15].

Lu et al. found that, in the initial concentration of 60 ppm and 200 ppm of benzene and toluene, the amount of toluene adsorbed in terms of the adsorbent mass unit is greater than the amount of adsorbed benzene [16]. In addition, Aivalioti et al. [17] have shown the greater adsorption potential of diatomaceous adsorbents in the removal of benzene, compared to toluene. Daifullah and Girgis [15] have found that the adsorption of benzene in terms of the adsorbent mass unit is more than toluene.

Su et al. in a previous study reported the adsorption potential of benzene and toluene to be 212 and 225 mg/g, using sodium hypochlorite-modified nanotubes at an initial concentration of 200 ppm, contact time of 240 minutes, and adsorbent concentration of 600 mg/L. Benzene adsorption capacity was greater than toluene [18]. This finding reveals that benzene and toluene adsorption by different adsorbents is dependent on the chemical properties and porosity of the adsorbent surface. Similar results have been provided by other researchers in previous articles [15].

The aim of this research project was to conduct batch experiments to study adsorption capacity, reaction kinetics, and the effects of critical operating parameters on benzene and toluene removal by CuO-NPs. Four factors including pH, CuO-NPs dose, contact time, and initial benzene and toluene concentration were used to survey the efficiency of CuO-NPs in benzene and toluene removal from aqueous environments. Furthermore, modeling of experimental data was performed by isotherm equations.

2. Materials and Methods

2.1. Materials. Benzene, toluene, and copper nitrate ($Cu(NO_3)_2{\cdot}3H_2O$) were supplied by Merck Co. (Germany). To prepare the stock solution, 2 mL of benzene and 2 mL of toluene (with a purity of 99.7%) were added to 1 L methanol. The homogeneous stock solution was completely sealed and stored in a volumetric flask until the daily solutions were prepared at different concentrations. A conventional method was applied to prepare CuO-NPs. First, distilled water was used to dissolve $Cu(NO_3)_2{\cdot}3H_2O$. The solution pH was set at 10 using Na_2CO_3 (1 M) through stirring. Then, the product was aged with stock liquor over 12 hours at room temperature. Filtration was performed to gather the product. Afterwards, it was rinsed with demineralized water, dried for 1 day at 60°C, and calcined at a temperature of 350°C for 4 hours [19].

2.2. Analysis. In this study, benzene and toluene concentrations were analyzed using a headspace-gas chromatograph (Agilent 7890 A, Palo Alto, CA, USA) with a flame ionization detector and a capillary column (thickness, 0.25 μm; length, 30 m; ID, 0.32 mm). For benzene and toluene measurements, the thermal program of the column was set at 40°C for 10 minutes, followed by a rise in temperature (temperature, 120°C; speed, 10°C/min) continuing for 2 minutes. The temperature of the injection site was fixed at 250°C, and 1 mL of the sample was injected into the device in the splitless mode. The gas chromatography effluent was transferred to an ionization source detector at 280°C through a 280°C transmission line. The analysis was performed in the selected ion monitoring mode. In addition, a Quanta-400F microscope, equipped with a field emission (KYKY-EM3900M, China) was used to perform scanning electron microscopy (SEM) of the prepared CuO-NPs on gold-coated samples. In order to determine the X-ray diffraction (XRD) pattern (CuK radiation; 40 kV; 30 mA), an advanced D8 diffractometer (Bruker, Germany) was used. In addition, a pH meter (WTW inoLab 7310) was employed to assess the solution pH.

2.3. Adsorption Experiments. In the present study, triplicate batch experiments were performed. Batch adsorption experiments were performed in flasks (250 mL) via magnetic stirring. We prepared 100 mL of benzene and toluene solution (initial dose, 10–200 mg/L) through dilution of the stock solution with distilled water; afterwards, it was moved to a beaker and placed on a magnetic stirrer.

We adjusted pH (range, 3–13) by using a solution containing 0.1 N of HCl or NaOH. Then, 0.1–0.8 g/L of synthesized CuO-NPs was added, and the suspension was stirred during 5–120 minutes. The samples were removed from the mixture with a micropipette after reaching the desired contact duration; then, the residual concentration of benzene and toluene was analyzed by GC method.

Adsorption kinetic experiments were performed with 250 mL beakers, containing 0.6 g of CuO-NPs and 100 mL of benzene and toluene (10, 20, 50, 100, and 200 mg/L) at pH of 7. After different intervals, we gathered and filtered the sample aliquots with syringe filters. Then, to determine the amount of the remaining contaminant, the aliquots were injected into the GC device. A similar procedure was applied for experiments on adsorption isotherms, with the exception that we used different concentrations of benzene and toluene solutions. The experiments were performed in triplicate under the same conditions to check the reproducibility of calculations; then, we measured the average values. The

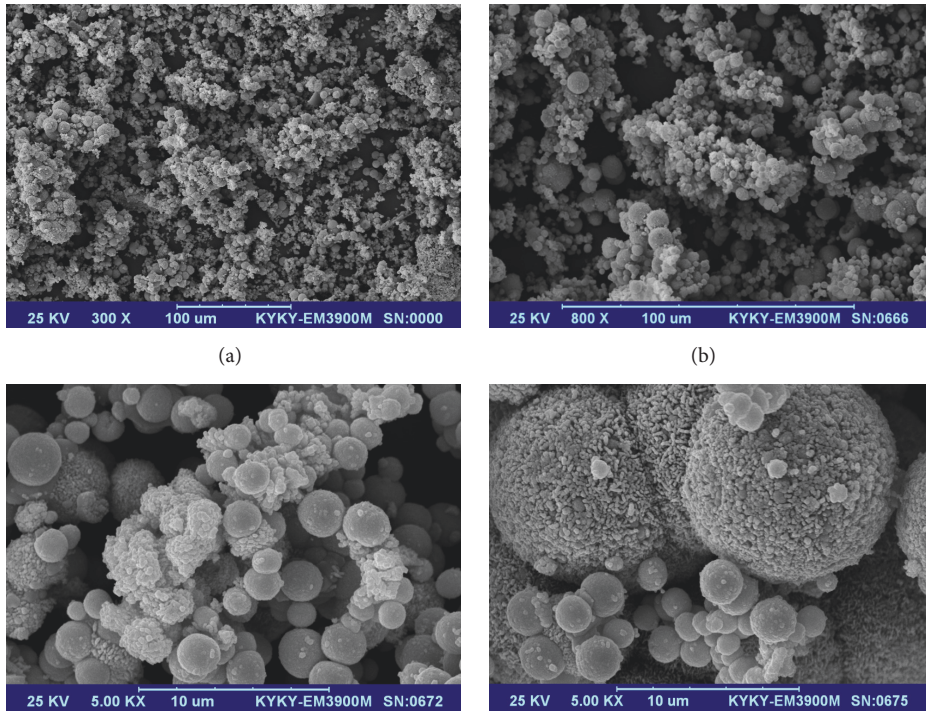

(a) (b) (c) (d)

Figure 1: SEM images of CuO nanoparticles.

amount of the adsorbed benzene and toluene q_e (mg/g) was calculated under different conditions:

$$q_e = \frac{(C_0 - C_e)V}{M}. \quad (1)$$

In this equation, C_0 is the initial concentration, C_e denotes the liquid-phase dose of benzene and toluene at equilibrium in mg/L, V denotes the solution volume (L), and M refers to the quantity of the adsorbent (g). Moreover, to determine the benzene and toluene removal percentage, the following formula was used:

$$\text{Removal efficiency, \%} = \frac{(C_i - C_e)}{C_i} \times 100, \quad (2)$$

where C_i denotes the initial dose of the pollutant and C_e is the effluent concentration in mg/L.

We carried out the experiments in duplicate to ensure the reproducibility of the findings; then, we measured the mean of 2 calculations. The equilibrium isotherm was demonstrated by the plot of equilibrium adsorption potential versus concentration at equilibrium.

3. Results and Discussion

3.1. Adsorbent Characterization. View of adsorbent used for removing benzene and toluene in this study was analyzed by SEM and XRD device. Figure 1 shows the order specified absorbent SEM of the adsorbent. An agglomeration of nanoscale particles with spherical and flower shapes is clearly observed. The average diameter of spherical CuO-NPs counted from the SEM images is about 148 nm. Figure 2 shows the XRD profile of the adsorbent (CuO-NPs). All 11 diffraction peaks at 2θ = 33°C, 36°C, 39°C, 49°C, 54°C, 59°C, 62°C, 66°C, 68°C, 73°C, and 75°C were indexed to (110), (002), (111), (202), (020), (202), (113), (311), (113), (311), and (004) planes, respectively, which are related to the monoclinic crystal phase of CuO-NPs; these values are comparable with those in JCPDS file for CuO (JCPDS, card number 45-0937).

3.2. Analysis of the Effect of Solution pH. The solution pH is a critical factor in the application of nanoadsorbents as support materials in the removal of various pollutants in the adsorption process [20–25]. Under different pH environments, transference of proton might take place on the surface of metal oxides, leading to adsorption in reaction pathways [26]. To determine the optimum solution pH, it was changed from 3 to 13 with an initial benzene/toluene dosage of 50 mg/L and an adsorbent concentration (CuO-NPs) of 0.4 g per 100 mL of solution. Figure 3 shows the effect of initial solution pH on benzene/toluene adsorption. It can be seen that, by increasing pH from 3 to 7, the removal efficiency increased from about 61.76% to 67.36% for benzene and 68.34% to 73.28% for toluene and continuous increasing of pH decreased the efficiency. The greatest adsorption potential was estimated to be 84.2 and 91.6 mg/g for benzene and toluene at a pH of 7, respectively. Under these conditions, the residual concentration of benzene was 16.32 mg/L and that of toluene was 13.36 mg/L. According to these results, the optimum pH was found to be 7 for benzene/toluene

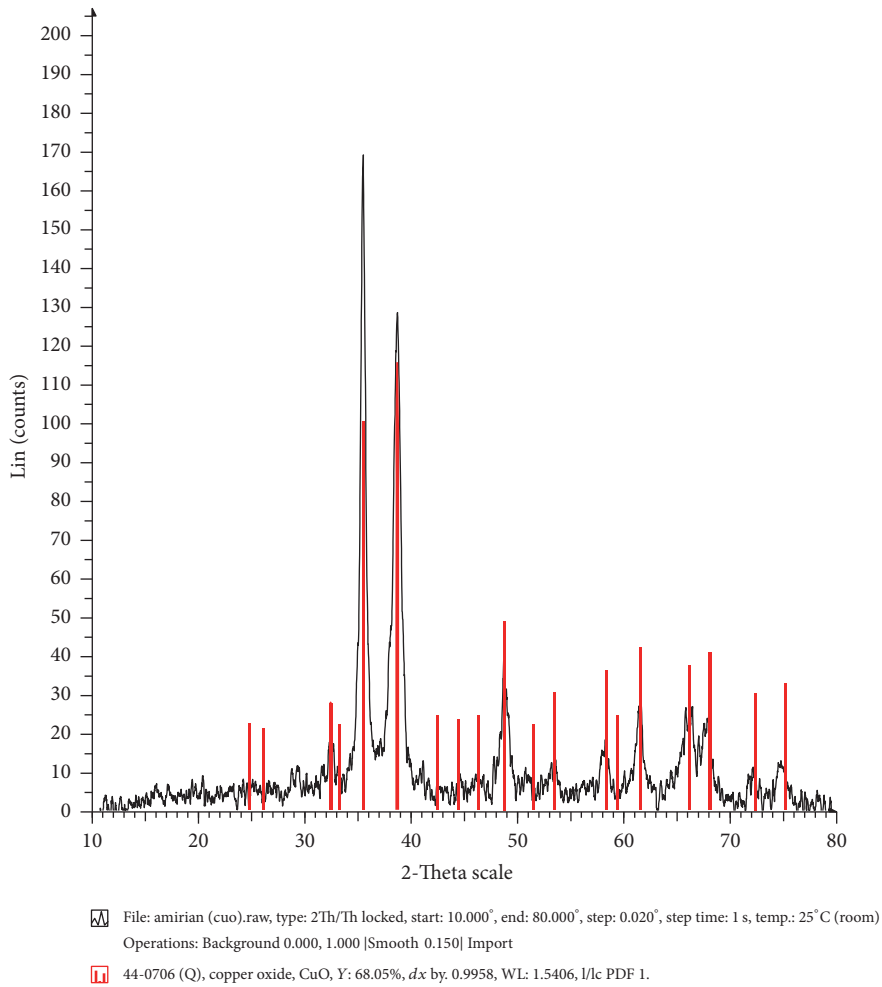

Figure 2: XRD patterns of CuO-NPs.

adsorption. Consequently, pH of 7 was considered optimal for the next steps.

3.3. Effect of CuO-NP Dose on Benzene/Toluene Adsorption. The adsorbent dose is a critical factor, as it can show the adsorbent's potential (CuO-NPs) for a specific initial concentration of benzene/toluene. Hence, to determine the impact of CuO-NPs dose on benzene/toluene adsorption, 0.1 to 0.8 g/L of the adsorbent was used in the experiments at pH of 7 and initial benzene/toluene concentration of 50 mg/L for 60 minutes. As presented in Figure 4, benzene/toluene removal efficiency is associated with CuO-NPs dosage in the solution. Based on the diagram, by increasing the concentration of the adsorbent from 0.1 to 0.6 g, the removal efficiency was enhanced from 62% to 93% for benzene and from 52% to 89% for toluene. Under these conditions, the residual concentration of benzene and toluene reached 3.29 and 5.22 mg/L, respectively.

Furthermore, as demonstrated in Figure 4, benzene/toluene removal capacity was rapidly enhanced by increasing the quantity of CuO-NPs from 0.1 to 0.6 g and from 0.6 to 0.8 g. We can explain this finding by resorting to the fact that sorption sites continue to be unsaturated in sorption, while the available sites grow in number by raising the adsorbent dosage [21]. Furthermore, it was found that further increase in dosage beyond 8 g/L rarely affected adsorption capacity of CuO-NPs (data not showed). Consequently, 0.6 g adsorbent was considered as the optimum dose.

In addition as presented in Figure 4, the equilibrium adsorption capacity of CuO-NPs decreased from 312.4 to 77.85 mg for benzene and 263.9 to 74.63 mg for toluene. On the other hand, the adsorbed benzene/toluene per gram of adsorbent reduced fast with a rise in CuO-NPs (maximum adsorption capacity, 312.4 mg/g for benzene and 263.9 mg/g for toluene at minimum adsorbent concentration of 0.1 g/L). This observation might be associated with the fixed benzene/toluene dosage (50 mg/L), producing active sites on the surface of CuO-NPs and increasing the adsorbent dosage due to aggregation of particles [27]; similar results have been reported by other researchers [21, 22, 24, 28].

3.4. Effects of Contact Time and Initial Benzene/Toluene Concentration. In the adsorption process, pollutant elimination from aqueous solutions is relative to the duration of

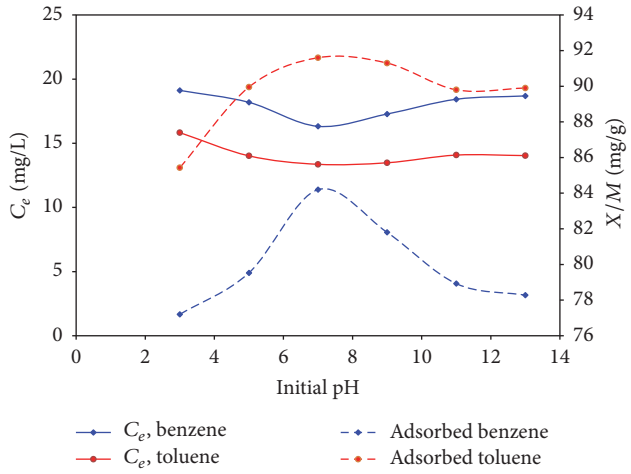

FIGURE 3: The effect of solution pH on benzene and toluene adsorption by CuO-NPs (CuO-NPs dose = 0.4 g/L, contact time = 60 min, and benzene and toluene concentration = 50 mg/L).

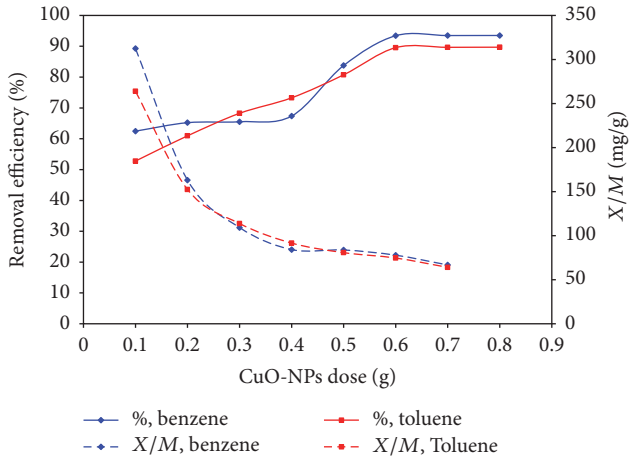

FIGURE 4: Effect of adsorbent dose on benzene and toluene adsorption by CuO-NPs (benzene/toluene concentration = 50 mg/L, initial pH = 7, and contact time = 60 min).

adsorbent-adsorbate contact [22, 29, 30]. Also, the initial concentration of solute is of remarkable importance due to its role in solid/liquid equilibrium. Hence, benzene/toluene removal by CuO-NPs was investigated as a function of contact duration. Accordingly, the effectiveness of contact duration in the adsorption of benzene/toluene on CuO-NPs was examined at a fixed pH of 7, CuO-NP dose of 0.6 g/L, and various benzene/toluene concentrations.

The analysis of the relationship between contact time and rate of adsorption in the studied pollutants by CuO-NPs at different concentrations is shown in Figures 5 and 6. As can be seen, at all concentrations tested, the highest removal efficiencies were observed in contact times of >40 minutes. Also, as presented in Figures 5 and 6, pollutant elimination improved by increasing the contact time at different initial concentrations of benzene/toluene. In fact, in the first 20 minutes, the adsorption rate was reported to be high (36–63% for benzene and 38–59% for toluene), followed by a slower rate of adsorption and finally equilibrium within 80 minutes. Hence, due to the fact that no significant increase occurs in removal efficiency after 80 minutes, the contact time of 80 minutes was considered as the optimal adsorption time (equilibrium time). The high removal rate of benzene/toluene during the first one-third of reaction time has been attributed to the interfacial bonding of adsorbate on the empty and ready-to-adsorb binding sites of adsorbent surface. Similar findings were reported by other researchers [25, 31].

The results regarding the effect of initial benzene/toluene concentration are shown in Figures 5 and 6. As can be clearly seen, rise in the initial pollutant concentration could increase the removal efficiency and adsorption capacity. For instance, with an initial benzene concentration of 10 mg/L (contact time, 80 min), removal efficiency reached more than 87.4% with an adsorption capacity of 14.57 mg/g, whereas, at an initial benzene concentration of 200 mg/L, the corresponding values were 94.87% and 316.23 mg/g, respectively; similar trends were obtained for toluene. Consequently, the removal of benzene/toluene by CuO-NPs depends on the concentration of the pollutant. The rise in adsorption capacity (q_e) by increasing the initial benzene/toluene concentration at fixed dose of adsorbent can be described by the increased driving force, associated with the concentration gradient [32]. In fact, the initial concentration of the pollutant molecules provides an important driving force to overcome the mass transfer resistance of all molecules between the aqueous and solid phases. Bulut et al. [33] observed that the amount of dye molecules adsorbed per unit mass of biosorbent increased with an increase in initial dye concentration from 50 to 250 mg/L. It is estimated that the binding sites of sorbent stay unsaturated during the biosorption mechanism.

3.5. Adsorption Kinetics. Adsorption kinetics are of great importance in the application of adsorbents in actual situations. Several models have been employed to describe and explain the mechanisms involved in the sorption process. In the present study, to assess the adsorption kinetics of benzene and toluene on CuO-NPs, we used different models. In the pseudo-first model, it is assumed that there is a direct relation between changes in the rate of adsorption of the solved substance and time [25, 34]. The linear form of the first-order kinetics is shown in

$$\ln(q_e - q_t) = \ln q_e - k_1 t, \tag{3}$$

where k_1 denotes the pseudo-first-order rate constant (1/minute), q_e represents the amount of adsorbed benzene and toluene at equilibrium (mg/g), q_t is the amount of adsorbed benzene and toluene at time t (mg/g), and t denotes time in minutes. Therefore, a plot of $\ln(q_e - q_t)$ versus t determines k_1 with respect to the slope and $\ln q_e$ with respect to the intercept of the plot.

The second-order kinetic model [21] is presented as follows:

$$\frac{t}{q_t} = \frac{1}{k_2 q_e^2} + \frac{t}{q_e}. \tag{4}$$

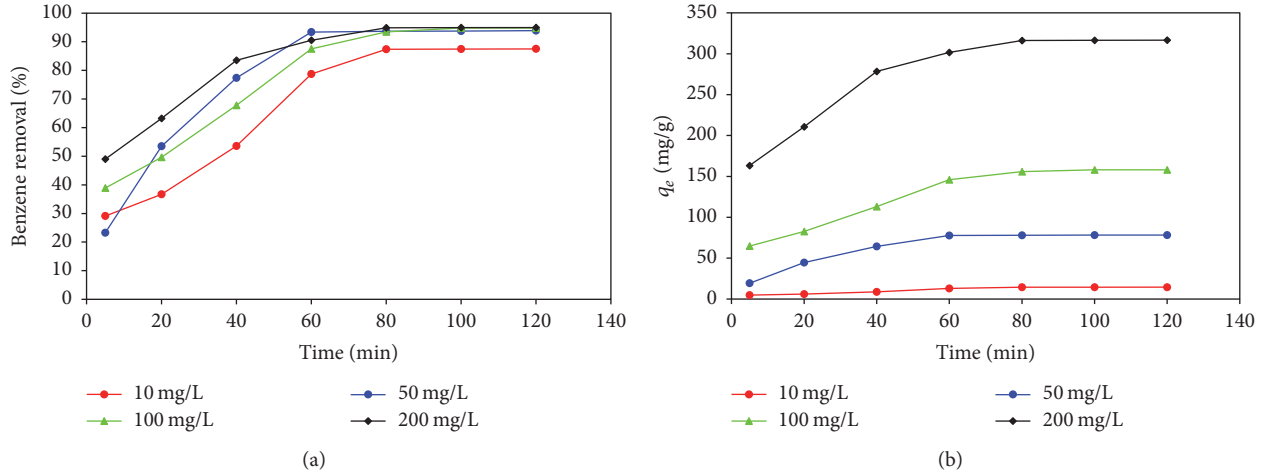

Figure 5: The effect of contact time on benzene adsorption by CuO-NPs ((a) percent removal efficiency, (b) adsorption capacity).

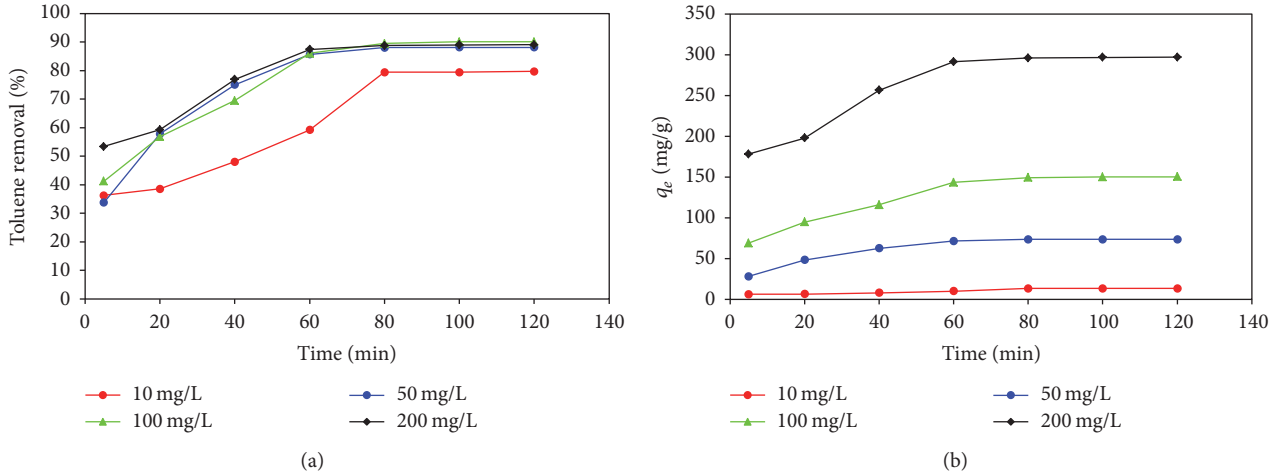

Figure 6: The effect of contact time on toluene adsorption by CuO-NPs ((a) percent removal efficiency, (b) adsorption capacity).

In this equation, k_2 represents the pseudo-second-order rate constant (g/mg/min), q_e denotes the amount of adsorbed benzene/toluene during equilibrium (mg/g), q_t denotes the amount of adsorbed benzene and toluene at time t (mg/g), and t refers to time in minutes. In case second-order kinetics were considered valid, a t/q_t versus t plot can indicate the linear correlation. In addition, the rate constants of k_2 and q_e can be measured with respect to the slope and intercept of the plot, respectively. This model can probably predict behaviors during the adsorption process and is in accordance with chemical sorption (stage of rate control). On the other hand, adsorption is assumed to be directed by chemical adsorption in the second-order kinetic model.

The intraparticle diffusion model is mathematically expressed as [35]

$$q_t = k_p t^{0.5} + C, \tag{5}$$

where k_p denotes the intraparticle diffusion rate constant in mg/g/min 0.5, C is the intraparticle diffusion constant in mg/g, t is time in minutes, and q_t is defined as before. By drawing q_t in terms of $t^{0.5}$, k_p and C can be obtained. In the present research, the intraparticle diffusion model was applied to determine the adsorption mechanism. As previously described by Weber and Morris [36], it should be noted that porosity and intraparticle diffusion influence the adsorption rate in a non-flow-agitated system.

The linear plots of pseudo-first-order, pseudo-second-order, and intraparticle diffusion models for benzene and toluene are illustrated in Figures 7–9. In addition, the values of reaction constants and correlation coefficients obtained from the linear plots are presented in Table 1. It is apparent from the values of correlation coefficients that fitness of the pseudo-second-order model is better as compared to pseudo-first-order model (the linear regression correlations (R^2) from pseudo-second-order model were higher than those from pseudo-first-order model). As reported by Pillewan et al. [37], in adsorption systems following pseudo-second-order models, a common mechanism is chemical adsorption, incorporating a chemical bond between the active adsorbent sites and adsorbate valence forces.

Table 1: Kinetic parameters for the adsorption of benzene/toluene by CuO-NPs for different concentrations at pH = 7.

C_0, mg/L	Pseudo-first-order			Pseudo-second-order			Intraparticle diffusion		
	k_1 (1/min)	q_e (mg/g)	R^2	k_2 (g/mg/min)	q_e, mg/g	R^2	k_p (g/mg/min$^{0.5}$)	C (mg/g)	R^2
Benzene									
10	0.0235	1056	0.8629	1.5511	0.0543	0.9441	1.3165	1.4322	0.9262
50	0.0398	38.66	0.6156	0.1912	0.0108	0.9922	6.876	13.179	0.871
100	0.0465	164.35	0.9476	0.0955	0.0055	0.9823	12.151	37.5	0.9407
200	0.0515	224.08	0.9149	0.0246	0.0029	0.9971	18.694	136.61	0.9061
Toluene									
10	0.021	9.39	0.8922	1.5549	0.063	0.9342	0.9983	2.7892	0.9055
50	0.037	40.07	0.8834	0.1322	0.0123	0.9975	5.251	23.492	0.8835
100	0.0453	109.51	0.9077	0.0709	0.006	0.9926	10.097	51.504	0.9335
200	0.0499	165.67	0.9003	0.024	0.0031	0.9926	15.521	146.66	0.8969

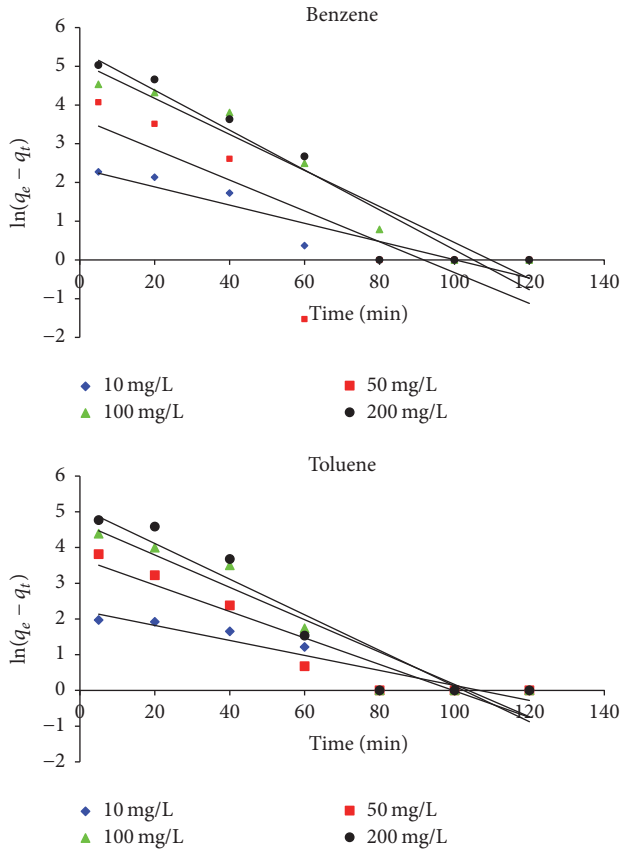

Figure 7: Pseudo-first-order kinetic plots for benzene/toluene adsorption on CuO-NPs at different initial concentration of benzene/toluene (adsorbent dose = 0.6 g/L, pH = 7).

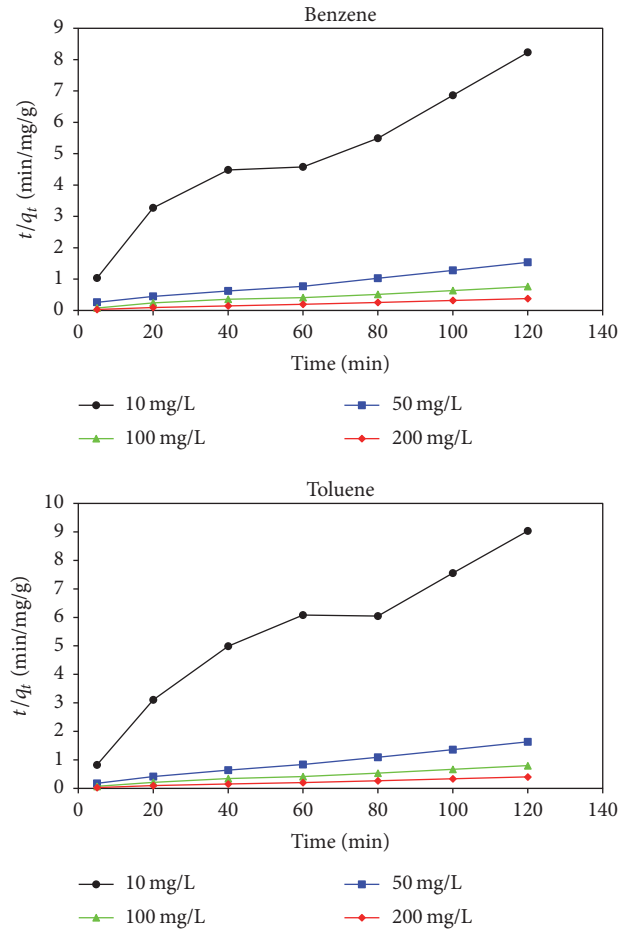

Figure 8: Pseudo-second-order kinetic plots for benzene and toluene adsorption on CuO-NPs at different initial concentration of benzene/toluene (adsorbent dose = 0.6 g/L, pH = 7).

Furthermore, the plot of the linear form of intraparticle diffusion model is presented in Figure 9. Also, the results of the analysis of parameters are demonstrated in Table 1. The R^2 values of the particle diffusion model are almost uniform, showing the greater contribution of adsorbate particle diffusion to constant rate analysis.

3.6. Equilibrium Adsorption Isotherm. Isotherms of adsorption are valuable curves to describe the adsorption equilibrium and provide a great deal of information to reveal the reciprocity between the adsorbent and adsorbate. On

Table 2: Isotherm parameters for adsorption of benzene/toluene onto CuO-NPs.

	Benzene			Toluene		
Langmuir isotherm	q_m (mg/g)	k_l (L/mg)	R^2	q_m (mg/g)	k_l (L/mg)	R^2
	100.24	0.1	0.9718	111.31	0.05	0.9826
Freundlich isotherm	k_f	n	R^2	k_f	n	R^2
	11.79	0.7	0.9836	5.88	0.76	0.9818
Temkin isotherm	k_T	B	R^2	k_T	B	R^2
	$1.79359E + 31$	0.0065	0.8678	$1.70366E + 52$	0.0079	0.9144
D-R isotherm	q_m	β	R^2	q_m	β	R^2
	6.08	0.0024	0.9812	5.84	0.0035	0.9782

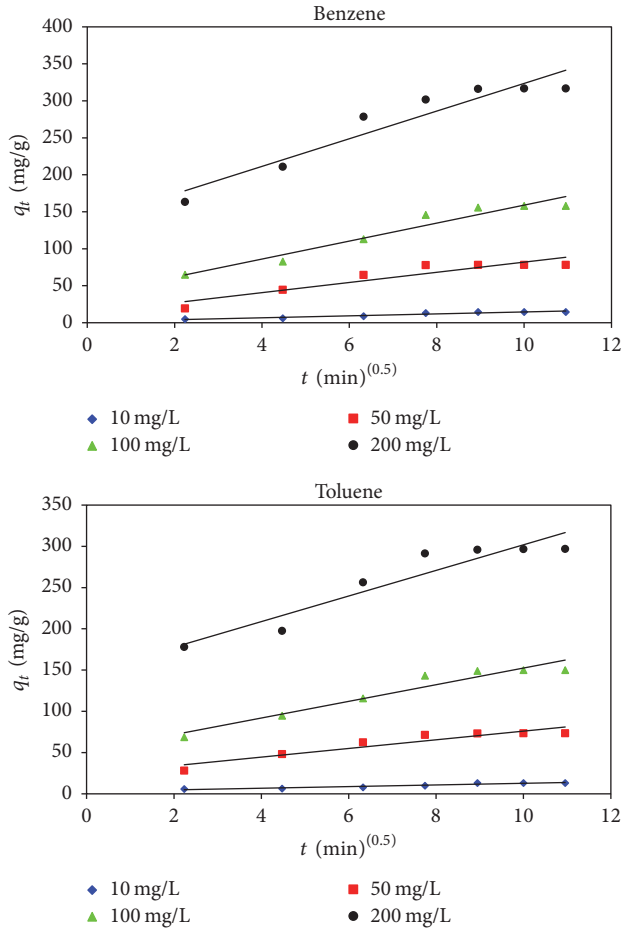

Figure 9: Intraparticle diffusion kinetic plots for benzene/toluene adsorption on CuO-NPs at different initial concentrations (adsorbent dose = 0.6 g/L, pH = 7).

the other hand, adsorption isotherms are adsorption properties and equilibrium data, which describe the reactions of pollutants with adsorbents and have a critical role in the optimization of adsorbent use [38].

As presented in Table 2, Langmuir, Freundlich, Temkin, and Dubinin-Radushkevich models were applied in order to examine the equilibrium isotherms for benzene/toluene adsorption on CuO-NPs and explain the equilibrium adsorption information. These models are applied to describe the adsorption mechanisms, surface adsorbent characteristics, adsorption affinity, and adsorption experimental data. Consequently, building an excellent correlation between equilibrium diagrams for optimization of conditions and designing adsorption systems is very important [39].

3.6.1. Langmuir Model. It is appropriate for monolayer adsorption on surfaces, consisting of a fixed quantity of identical sorption sites. On the other hand, this model includes assumptions such as monolayer adsorption, surface uniformity, and removal of the interaction of the adsorbed molecules. For monolayer adsorption, the Langmuir equation is as follows:

$$q_e = \frac{q_m k_l C_e}{1 + k_l C_e}. \quad (6)$$

In this equation, q_e denotes the quantity of adsorbed benzene/toluene per unit mass of CuO-NPs as the adsorbent (mg/g), C_e denotes the solution's concentration at equilibrium (mg/L), and q_m refers to the maximum quantity of benzene/toluene for developing a monolayer on CuO-NPs (mg/g). It is possible to reset the Langmuir model in a linear form to facilitate plotting and determine the Langmuir constants (k_l), as well as the optimal monolayer adsorption potential of the adsorbent (q_m). Also, q_m and k_l are measured based on the linear plot ($1/q_e$ versus $1/C_e$):

$$\frac{1}{q_e} = \frac{1}{q_m} + \frac{1}{q_m k_l}\frac{1}{C_e}. \quad (7)$$

3.6.2. Freundlich Model. In this model, the assumption is that adsorption takes place on heterogeneous surfaces. Based on this model, the process is defined as follows [40]:

$$q_e = k_f C_e^{1/n}. \quad (8)$$

In this equation, k_f and $1/n$ denote the characteristics of Freundlich constants, k_f represents the adsorption potential of the adsorbent, and n represents the intensity of adsorption. The equilibrium constants were examined with respect to the intercept and slope of the linear plot ($\ln q_e$ versus $\ln C_e$), respectively, according to the experimental information.

3.6.3. Temkin Model. In this model, the assumption is that reduced sorption heat is linear, and binding energy distribution is uniform (up to the highest binding energy).

It considers indirect adsorbate-adsorbent interactions and suggests a linear decline in adsorption heat of all molecules inside the layer due to these interactions. Temkin model is normally as follows:

$$q_e = B \ln k_T + B \ln C_e, \quad (9)$$

where k_T and B are measured based on a linear plot of q_e versus $\ln C_e$, k_T denotes the equilibrium binding constant (L/mg; the highest binding energy), and B is associated with the adsorption heat.

3.6.4. Dubinin-Radushkevich Model. This model is frequently applied to examine the porosity and free adsorption energy. The linear form of Dubinin-Radushkevich (D-R) model is as follows:

$$\log q_e = \ln q_m - \beta\varepsilon^2. \quad (10)$$

In this equation, β denotes a constant associated with the mean free adsorption energy per mole of the adsorbate (mol^2/KJ^2), q_m refers to the theoretical saturation potential (mg/g), and ε represents the Polanyi potential [21, 41].

The relationship between the amount of adsorbed benzene and toluene and their equilibrium concentrations was described by the four equations of adsorption isotherm, as follows: Langmuir, Freundlich, Dubinin-Radushkevich (D-R), and Temkin, and the best-fit equilibrium model was established based on the linear regression correlation coefficients, R^2. The values of R^2 from Table 2 show that the Freundlich and Langmuir models give a good fit to the sorption isotherm for benzene and toluene onto CuO-NPs, respectively.

4. Conclusion

In the present study, CuO-NPs were successfully applied for benzene/toluene removal from aqueous environments. Based on the findings, the removal percentage was dependent on the solution pH, amount of CuO-NPs as the adsorbent, initial benzene/toluene dosage, and pollutant-adsorbent contact time. The maximum removal efficiency of CuO-NPs for benzene and toluene was observed at a pH of 7. Also, based on the findings, CuO-NPs could remove 98.7–25.41% of benzene and 92.5–35.2% of toluene from solutions with an initial dosage of 10–200 mg/L and contact duration of 1 hour. By increasing CuO-NPs and duration of contact, the removal percentage of benzene and toluene improved. According to the results, the sorption data fitted into the Langmuir, Freundlich, Temkin, and Dubinin-Radushkevich models. Also, benzene well fitted into the Freundlich model, and toluene well fitted into the Langmuir model. Based on the analyses, adsorption follows pseudo-second-order kinetics.

Conflicts of Interest

The authors declare that there are no conflicts of interest regarding the publication of this manuscript.

Acknowledgments

This article is derived from the Ph.D. thesis of Ms. L. Mohammadi and all authors are grateful to the Zahedan University of Medical Sciences for the financial support of this study (Project no. 7391). Furthermore, all authors wish to thank Dr. Hossein Kamani, Dr. Ferdos Kord Mostafapour, and Ms. Sh. Sargazi for their support during the analysis of experiments.

References

[1] A. R. Bielefeldt and H. D. Stensel, "Evaluation of biodegradation kinetic testing methods and longterm variability in biokinetics for BTEX metabolism," *Water Research*, vol. 33, no. 3, pp. 733–740, 1999.

[2] L. Mohammadi, *BTEX and chlorophenols compounds removal from synthetic sollutions by heterogenous catalytic ozonation using FeO, CuO and MgO nanoparticles [Ph.D. desertaion]*, Zahedan University of Medical Sciences, (in Persian), 2017.

[3] X. Fu, X. Gu, S. Lu et al., "Enhanced degradation of benzene in aqueous solution by sodium percarbonate activated with chelated-Fe(II)," *Chemical Engineering Journal*, vol. 285, pp. 180–188, 2016.

[4] N. Kang and I. Hua, "Enhanced chemical oxidation of aromatic hydrocarbons in soil systems," *Chemosphere*, vol. 61, no. 7, pp. 909–922, 2005.

[5] B. Bina, H. Pourzamani, A. Rashidi, and M. M. Amin, "Ethylbenzene removal by carbon nanotubes from aqueous solution," *Journal of Environmental and Public Health*, vol. 2012, Article ID 817187, 8 pages, 2012.

[6] A. K. Mathur, C. B. Majumder, and S. Chatterjee, "Combined removal of BTEX in air stream by using mixture of sugar cane bagasse, compost and GAC as biofilter media," *Journal of Hazardous Materials*, vol. 148, no. 1-2, pp. 64–74, 2007.

[7] J. M. M. D. Mello, H. de Lima Brandão, A. A. U. de Souza, A. da Silva, and S. M. D. A. G. U. de Souza, "Biodegradation of BTEX compounds in a biofilm reactor-Modeling and simulation," *Journal of Petroleum Science and Engineering*, vol. 70, no. 1-2, pp. 131–139, 2010.

[8] M.-Q. Jiang, Q.-P. Wang, X.-Y. Jin, and Z.-L. Chen, "Removal of Pb(II) from aqueous solution using modified and unmodified kaolinite clay," *Journal of Hazardous Materials*, vol. 170, no. 1, pp. 332–339, 2009.

[9] A. Afkhami and R. Moosavi, "Adsorptive removal of Congo red, a carcinogenic textile dye, from aqueous solutions by maghemite nanoparticles," *Journal of Hazardous Materials*, vol. 174, no. 1–3, pp. 398–403, 2010.

[10] M. Yang, J. He, X. Hu, C. Yan, and Z. Cheng, "CuO nanostructures as quartz crystal microbalance sensing layers for detection of trace hydrogen cyanide gas," *Environmental Science and Technology*, vol. 45, no. 14, pp. 6088–6094, 2011.

[11] A. R. Türker, "New sorbents for solid-phase extraction for metal enrichment," *Clean-Soil Air Water*, vol. 35, no. 6, pp. 548–557, 2007.

[12] W.-X. Zhang, "Nanoscale iron particles for environmental remediation: an overview," *Journal of Nanoparticle Research*, vol. 5, no. 3-4, pp. 323–332, 2003.

[13] K. E. Engates and H. J. Shipley, "Adsorption of Pb, Cd, Cu, Zn, and Ni to titanium dioxide nanoparticles: Effect of particle size, solid concentration, and exhaustion," *Environmental Science and Pollution Research*, vol. 18, no. 3, pp. 386–395, 2011.

[14] C. A. Martinson and K. J. Reddy, "Adsorption of arsenic(III) and arsenic(V) by cupric oxide nanoparticles," *Journal of Colloid and Interface Science*, vol. 336, no. 2, pp. 406–411, 2009.

[15] A. A. M. Daifullah and B. S. Girgis, "Impact of surface characteristics of activated carbon on adsorption of BTEX," *Colloids and Surfaces A: Physicochemical and Engineering Aspects*, vol. 214, no. 1-3, pp. 181–193, 2003.

[16] C. Lu, F. Su, and S. Hu, "Surface modification of carbon nanotubes for enhancing BTEX adsorption from aqueous solutions," *Applied Surface Science*, vol. 254, no. 21, pp. 7035–7041, 2008.

[17] M. Aivalioti, I. Vamvasakis, and E. Gidarakos, "BTEX and MTBE adsorption onto raw and thermally modified diatomite," *Journal of Hazardous Materials*, vol. 178, no. 1-3, pp. 136–143, 2010.

[18] F. Su, C. Lu, and S. Hu, "Adsorption of benzene, toluene, ethylbenzene and p-xylene by NaOCl-oxidized carbon nanotubes," *Colloids and Surfaces A: Physicochemical and Engineering Aspects*, vol. 353, no. 1, pp. 83–91, 2010.

[19] K. Zhou, R. Wang, B. Xu, and Y. Li, "Synthesis, characterization and catalytic properties of CuO nanocrystals with various shapes," *Nanotechnology*, vol. 17, no. 15, pp. 3939–3943, 2006.

[20] E. Bazrafshan, P. Amirian, A. H. Mahvi, and A. Ansari-Moghaddam, "Application of adsorption process for phenolic compounds removal from aqueous environments: a systematic review," *Global Nest Journal*, vol. 18, no. 1, pp. 146–163, 2016.

[21] E. Bazrafshan, F. Kord Mostafapour, S. Rahdar, and A. H. Mahvi, "Equilibrium and thermodynamics studies for decolorization of Reactive Black 5 (RB5) by adsorption onto MWCNTs," *Desalination and Water Treatment*, vol. 54, no. 8, pp. 2241–2251, 2015.

[22] E. Bazrafshan, A. A. Zarei, H. Nadi, and M. A. Zazouli, "Adsorptive removal of methyl orange and reactive red 198 dyes by moringa peregrina ash," *Indian Journal of Chemical Technology*, vol. 21, no. 2, pp. 105–113, 2014.

[23] E. Bazrafshan, M. Ahmadabadi, and A. H. Mahvi, "Reactive red-120 removal by activated carbon obtained from cumin herb wastes," *Fresenius Environmental Bulletin*, vol. 22, no. 2a, pp. 584–590, 2013.

[24] E. Bazrafshan, F. K. Mostafapour, and A. H. Mahvi, "Phenol removal from aqueous solutions using pistachio-nut shell ash as a low cost adsorbent," *Fresenius Environmental Bulletin*, vol. 21, no. 10, pp. 2962–2968, 2012.

[25] F. Kord Mostafapour, E. Bazrafshan, M. Farzadkia, and S. Amini, "Arsenic removal from aqueous solutions by salvadora persica stem ash," *Journal of Chemistry*, vol. 2013, Article ID 740847, 8 pages, 2013.

[26] E. Bazrafshan, F. K. Mostafapour, A. R. Hosseini, A. Raksh Khorshid, and A. H. Mahvi, "Decolorisation of reactive red 120 dye by using single-walled carbon nanotubes in aqueous solutions," *Journal of Chemistry*, vol. 2013, Article ID 938374, 8 pages, 2013.

[27] T. Calvete, E. C. Lima, N. F. Cardoso, S. L. P. Dias, and F. A. Pavan, "Application of carbon adsorbents prepared from the Brazilian pine-fruit-shell for the removal of Procion Red MX 3B from aqueous solution—kinetic, equilibrium, and thermodynamic studies," *Chemical Engineering Journal*, vol. 155, no. 3, pp. 627–636, 2009.

[28] E. Bazrafshan, D. Balarak, A. H. Panahi, H. Kamani, and A. H. Mahvi, "Fluoride removal from aqueous solutions by cupricoxide nanoparticles," *Fluoride*, vol. 49, no. 3, pp. 233–244, 2016.

[29] E. Bazrafshan, A. A. Zarei, and F. K. Mostafapour, "Biosorption of cadmium from aqueous solutions by Trichoderma fungus: kinetic, thermodynamic, and equilibrium study," *Desalination and Water Treatment*, vol. 57, no. 31, pp. 14598–14608, 2016.

[30] P. Loganathan, S. Vigneswaran, and J. Kandasamy, "Enhanced removal of nitrate from water using surface modification of adsorbents—a review," *Journal of Environmental Management*, vol. 131, pp. 363–374, 2013.

[31] B. Saha, K. E. Taylor, J. K. Bewtra, and N. Biswas, "Laccase-catalyzed removal of diphenylamine from synthetic wastewater," *Water Environment Research*, vol. 80, no. 11, pp. 2118–2124, 2008.

[32] E. Bekhradinassab and S. Sabbaghi, "Removal of nitrate from drinking water using nano SiO2-FeOOH-Fe core-shell," *Desalination*, vol. 347, pp. 1–9, 2014.

[33] Y. Bulut, N. Gözübenli, and H. Aydin, "Equilibrium and kinetics studies for adsorption of direct blue 71 from aqueous solution by wheat shells," *Journal of Hazardous Materials*, vol. 144, no. 1-2, pp. 300–306, 2007.

[34] N. Öztürk and T. E. Bektaş, "Nitrate removal from aqueous solution by adsorption onto various materials," *Journal of Hazardous Materials*, vol. 112, no. 1-2, pp. 155–162, 2004.

[35] J. Wu and H.-Q. Yu, "Biosorption of 2,4-dichlorophenol by immobilized white-rot fungus Phanerochaete chrysosporium from aqueous solutions," *Bioresource Technology*, vol. 98, no. 2, pp. 253–259, 2007.

[36] W. J. Weber and J. C. Morris, "Advances in water pollution research: removal of biologically resistant pollutants from waste waters by adsorption," in *Proceedings of the International Conference on Water Pollution Symposium*, vol. 2, pp. 231–266, Pergamon, Oxford, UK, 1962.

[37] P. Pillewan, S. Mukherjee, T. Roychowdhury, S. Das, A. Bansiwal, and S. Rayalu, "Removal of As(III) and As(V) from water by copper oxide incorporated mesoporous alumina," *Journal of Hazardous Materials*, vol. 186, no. 1, pp. 367–375, 2011.

[38] Z. Yang, H. Yi, X. Tang et al., "Potential demonstrations of 'hot spots' presence by adsorption-desorption of toluene vapor onto granular activated carbon under microwave radiation," *Chemical Engineering Journal*, vol. 319, pp. 191–199, 2017.

[39] S.-L. Hii, S.-Y. Yong, and C.-L. Wong, "Removal of rhodamine B from aqueous solution by sorption on Turbinaria conoides (Phaeophyta)," *Journal of Applied Phycology*, vol. 21, no. 5, pp. 625–631, 2009.

[40] S. Khorramfar, N. M. Mahmoodi, M. Arami, and K. Gharanjig, "Dye removal from colored textile wastewater using tamarindus indica hull: adsorption isotherm and kinetics study," *Journal of Color Science and Technology*, vol. 3, pp. 81–88, 2009.

[41] M. M. Montazer, P. Rabbani, A. Abdolali, and A. R. Keshtkar, "Kinetics and equilibrium studies on biosorption of cadmium, lead, and nickel ions from aqueous solutions by intact and chemically modified brown algae," *Journal of Hazardous Materials*, vol. 185, no. 1, pp. 401–407, 2011.